

RSC Advances



This is an *Accepted Manuscript*, which has been through the Royal Society of Chemistry peer review process and has been accepted for publication.

Accepted Manuscripts are published online shortly after acceptance, before technical editing, formatting and proof reading. Using this free service, authors can make their results available to the community, in citable form, before we publish the edited article. This *Accepted Manuscript* will be replaced by the edited, formatted and paginated article as soon as this is available.

You can find more information about *Accepted Manuscripts* in the [Information for Authors](#).

Please note that technical editing may introduce minor changes to the text and/or graphics, which may alter content. The journal's standard [Terms & Conditions](#) and the [Ethical guidelines](#) still apply. In no event shall the Royal Society of Chemistry be held responsible for any errors or omissions in this *Accepted Manuscript* or any consequences arising from the use of any information it contains.

A chemiluminescence sensor for determination of lysozyme using magnetic graphene oxide multi-walled carbon nanotubes surface molecularly imprinted polymers

Yanhui Wang, Huimin Duan, Leilei Li, Xiaojiao Wang, Jianbo Li, Yanan Bu, Chuannan Luo*

Key Laboratory of Chemical Sensing & Analysis in Universities of Shandong (University of Jinan), School of Chemistry and Chemical Engineering, University of Jinan, Jinan 250022, China

Abstract

In this paper, a new chemiluminescence (CL) sensor possessing high selectivity and sensitivity was established for determination of lysozyme using magnetic graphene oxide-multi-walled carbon nanotubes surface molecularly imprinted polymer (MGO-MWCNTs/SMIP). The MGO-MWCNTs/SMIP was characterized by X-ray Diffraction (XRD), Fourier Transform Infrared spectra (FT-IR) and Scanning Electron Microscopy (SEM), and the maximum adsorption capacity of MGO-MWCNTs/SMIP to lysozyme was researched to be 140 mg/g. The MGO-MWCNTs/SMIP was fixed into glass tube and was connected to the chemiluminescent analyzer. Then MGO-MWCNTs/SMIP-flow injection chemiluminescence (MGO-MWCNTs/SMIP-CL) sensor based on luminol-NaOH-H₂O₂ CL system for the determination of lysozyme was established. The proposed sensor with high selectivity and sensitivity responded linearly to the concentration of lysozyme over the range 5.04×10^{-9} - 4.27×10^{-7} g/mL and the detection limit was 1.90×10^{-9} g/mL (3 δ). The recoveries were ranging from 98% to 111% when determining lysozyme in eggs, and the result was satisfactory. The advantageous properties of sensor hold the potential to be applied in protein analysis, analogizing to biological analysis.

Key words: lysozyme; magnetic graphene-oxide; surface molecular imprinting; flow injection chemiluminescence; multi-walled carbon nanotubes

1. Introduction

As a basic enzyme which can hydrolyze mucopolysaccharide of the pathogens [1-2], lysozyme widely exists in most living body [3]. Lysozyme plays an important role in immune regulation aspects of human and is closely related to human health [4] with good antibacterial,

Corresponding author: Tel.: +860531 89736065. E-mail address: chm_yfl518@163.com

30 anti-inflammatory and anti-virus etc [5]. For now, lysozyme is mainly used in biochemical research
31 and has multiple applications in clinical, such as the treatment of herpes and warts [6-9]. So far,
32 some methods such as ion exchange method [10] and resonance light scattering method [11-12] etc
33 have been used for determination of lysozyme. However, these methods suffer from poor selectivity,
34 low sensitivity, poor anti-interference ability and expensive equipment. Therefore, development of a
35 novel method for lysozyme detection is very important. Recent years, surface molecules imprinting
36 (SMIP) technique with good selectivity has received much more attention. Molecularly imprinting
37 refers to the technology that prepares the polymer with selective recognition ability to target
38 molecular. Deng [13] had synthesized a copper ion selective membrane by surface-modified
39 molecular imprinting. And the adsorption selectivity of the ion imprinted membrane was increased.
40 Zayats [14] had obtained maltose imprinting in hydrogels by surface molecules imprinting technique
41 and the recognition of protein was tuned at the molecular level.

42 Flow Injection (FI) is a rapid online analytical technique [15]. Chemiluminescence (CL)
43 technology has the advantages of high sensitivity and wide linear range etc [16]. The FI-CL was
44 established with combination of these two methods. This method has the merits of high sensitivity
45 and wide linear range [17], and it is widely used in biology [18], pharmacy [19], environmental
46 science [20] and many other areas. Because of poor selectivity, FI-CL could not be directly used in
47 analyzing complex samples.

48 The combination of SMIP with high specific recognition and FI-CL with high-sensitivity in the
49 establishing the novel sensor has great significance. Interference from coexisting substances and
50 complex sample matrices was eliminated. Thereby, the anti-jamming capability of surface molecules
51 imprinting chemiluminescence (SMIP-CL) analysis was substantially strengthened.

52 In this work, using MGO-MWCNTs as the supporting material, the lysozyme
53 MGO-MWCNTs/SMIP was obtained. Due to the presence of MWCNTs, specific surface area of GO
54 were increased obviously and site of action were increased accordingly. And the agglomeration of
55 GO was reduced by the existence of MWCNTs. With the advantages of easy separation property of
56 magnetic Fe_3O_4 nanoparticles, high adsorption ability of GO-MWCNTs and excellent specificity
57 recognition of SMIP, the overall performance of MGO-MWCNTs/SMIP was increased dramatically.
58 And then, the adsorption properties of the polymers were studied. Then, the
59 MGO-MWCNTs/SMIP-CL sensor was constructed with high selectivity and high sensitivity and the

60 FI-CL analytical sensor for determination of lysozyme was established.

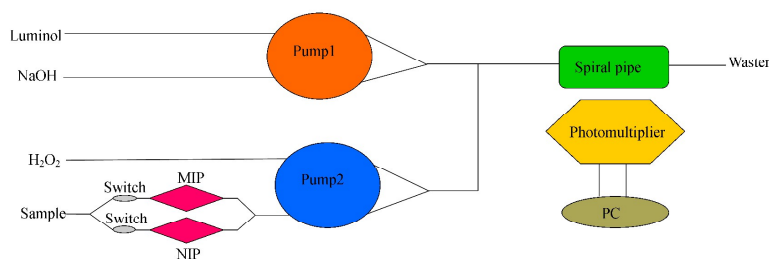
61 2. Materials and methods

62 2.1 Reagents

63 All the chemicals were of analytical reagent grade unless otherwise stated. Double-distilled
 64 water was used throughout this work. Lysozyme, acrylamide, methacrylic acid were purchased from
 65 Sinopharm Chemical Reagent Company (China). MWCNTs were purchased from Beijing Daojin
 66 Technology Company (China). Graphite was purchased from Tianjin Hongyan Chemical Reagent
 67 (China). 3-(methacryloyloxy) propyl trimethoxysilane (MPS), N,N'-methylene-bis-acrylamide,
 68 Diethylaminoethyl methacrylate (DMAEMA), Ethylene glycol dimethacrylate (EGDMA), N,N,N',
 69 N',-tetramethylethylenediamine were purchased from Aladdin Reagent Company (China).

70 2.2 Apparatus

71 The IFFM-E flow injection CL analyzer was purchased from Xi'an Remex Electronic
 72 Instrument High-Tech Ltd. The schematic of Luminol-NaOH-H₂O₂ CL system used in this study was
 73 shown in Fig. 1. The FI-CL analyzer was equipped with an automatic injection system and a detector.
 74 All of the components were connected with the flow system using polytetrafluoroethylene tube (0.8
 75 mm i.d.). The CL signal was analyzed with a personal computer.



76
 77 Fig. 1 The schematic of flow injection chemiluminescence system.

78 2.3 Preparation of MGO-MWCNTs/SMIP of lysozyme

79 GO was prepared according to the reported procedure from natural graphite powder by a
 80 modified hummers method [21]. Firstly, 1.0 g graphite powder was added into 500 mL three-necked
 81 flask. Then, 200 mL mixed acid solution (180 mL H₂SO₄ + 20 mL HNO₃ solution) was added into
 82 the flask, cooled by immersion in an ice bath and stirred for 0.5 h. Subsequently, 6.0 g KMnO₄ was
 83 slowly added and the reaction was carried out for 2 h while the temperature was kept to be 90 °C. In
 84 this process, the condensed city water was continuously for 12 h. In the hood, the ice bath was then
 85 removed and H₂O₂ was slowly dropwised added until the reaction was completed. The solution was

86 kept stirring until no gas generation. The final product was then centrifuged, washed twice with 30
87 mL 0.2 mol /L HCl solution and several times with 95% ethanol. Finally, the product was dried in
88 vacuum and brown GO was obtained.

89 GO-MWCNTs composites were obtained by using a previously reported procedure [22] with
90 modification. 1.0 g MWCNTs was dissolved in 70 mL HNO₃ solution (65~68 wt.%). The suspension
91 was stirred and refluxed for 11 h, and the temperature was kept below 75 °C. The product was
92 washed with distilled water until pH=6.5. The product was dried under a vacuum environment for 10
93 h at 80 °C. 0.3 g GO was stripped in 80 mL ethanol-water mixture (*V:V*=1:1) less than 3 h by
94 sonication. 0.4 g acidified MWCNTs was added to the alcohol-water solution at room temperature.
95 Then, the mixed solution was sonicated for 30 min. The solution was transferred to a 200 mL
96 teflon-lined stainless steel autoclave and maintained at 200 °C for 6 h. Thereafter, the product was
97 cooled to room temperature. The black cylindrical product was achieved and was washed seven
98 times with ethanol. Finally, the product of GO-MWCNTs was gained after drying at 60 °C under
99 vacuum.

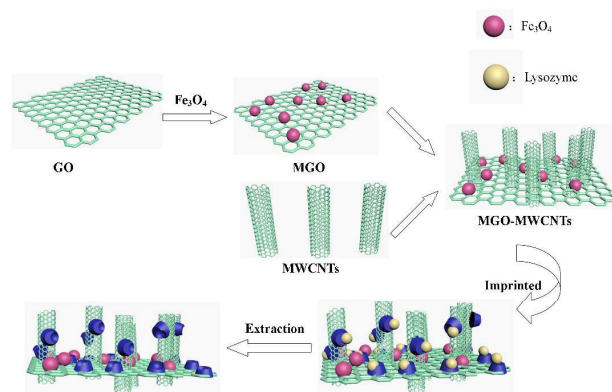
100 MGO-MWCNTs composites were synthesized by using a previously reported procedure [23].
101 50 mg GO-MWCNTs was dissolved in 30 mL ultrapure water and ultrasonic dispersing 0.5 h. 50 mg
102 FeCl₃ and 35 mg FeCl₂ were added into this solution and supplemented with 20 mL ultrapure water.
103 Under the protection of N₂, the solution was stirred and heated at 90 °C. NH₃·H₂O (28%) was added
104 into the solution until pH =9.0 and the solution was heated with stirring for 0.5 h. the solution was
105 separated with a magnet after heating and cooling to room temperature, washed twice with ethanol
106 and dried in a vacuum oven.

107 In this experiment, 0.3 g magnetic nanoparticles were added into a mixed solution (2 mL MPS
108 and 20 mL anhydrous toluene). Under the protection of N₂, the solution was refluxed for 12 h.
109 Finally, the product was collected by an external magnetic field, washed with ultrapure water and
110 obtained the product of silane modification.

111 Subsequently, 16 mg N,N-methylene bisacrylamide ,32.6 mg acrylamide, 0.1 mL methacrylate,
112 0.1 mL DMAEMA, 0.1 mL EGDMA, 32 mg lysozyme and 25 mL phosphate buffer solution (PBS,
113 pH=7.47, *c*: 0.01 mol/L) were added into 250 mL iodine flask and sonicated. Then, 120 mg
114 MGO-MWCNTs was dissolved in 15 mL ethanol and 5 mL PBS solution by ultrasonication. Then,
115 two solutions were mixed quickly and shocked for 1 h at 25 °C, then 30 mg (NH₄)₂S₂O₈, 0.4 mL

116 N,N,N,N,-tetramethylethylenediamine and 15 mg FeSO_4 were added into this solution. Subsequently,
 117 solution was shocked under nitrogen protection for 2 h at 25 °C. The product was washed twice with
 118 distilled water. In order to remove the unreacted monomers and the template molecule, the product
 119 was washed by NaCl (0.5mol/L) solution under ultrasonication. In the next step, to remove excess
 120 NaCl, the product was washed twice with distilled water and dried at 60 °C.

121 The MGO-MWCNTs/SNIP was obtained using the same way without the addition of lysozyme.
 122 The preparation process of MGO-MWCNTs/SMIP was shown in Fig. 2.



123
 124 Fig. 2 The preparation process of MGO-MWCNTs/SMIP.

125 2.4 Adsorption tests of MGO-MWCNTs/SMIP and MGO-MWCNTs/SNIP

126 MGO-MWCNTs/SMIP and MGO-MWCNTs/SNIP were added into the lysozyme solution for
 127 adsorption under the same conditions. The same volume of lysozyme solution was taken for test at
 128 different times to get the adsorption capacity. And a series of lysozyme standard solutions with
 129 different concentrations were prepared, and the same amounts of SMIP and SNIP were added into
 130 the solutions for adsorption of the lysozyme.

131 2.5 Procedure for determination of lysozyme

132 The schematic for the CL sensor was shown in Fig. 1 and specific experimental steps were
 133 shown as follows:

134 (1) Enrichment of lysozyme. Deputy pump (pump 1) stopped working. The injection valve was in
 135 the sampling position and the main pump (pump 2) transferred lysozyme solution flowing through
 136 the column of MGO-MWCNTs/SMIP for 60 s. The lysozyme was absorbed by
 137 MGO-MWCNTs/SMIP.

138 (2) Removing of residual impurities. Pump 1 stopped working, the injection valve was at the

139 sampling location and the Pump 2 transferred water to wash other substances except for lysozyme.

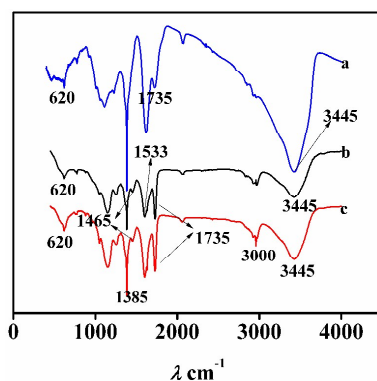
140 (3) Determination of lysozyme. Pump 2 and Pump 1 were started and the injector valve was in the
141 injection position. H_2O_2 and luminol solution flowed together in the column of
142 MGO-MWCNTs/SMIP for 50 s and reacted with lysozyme which generated a CL signal.

143 (4) Cleaning of the MGO-MWCNTs/SMIP column. Pump 1 stopped working and the injection
144 valve was in the sampling position. The main pump transferred water through the column of
145 MGO-MWCNTs/SMIP for 70 s. The residue was washed away from the column of
146 MGO-MWCNTs/SMIP for the test again.

147 3. Results and discussion

148 3.1 Characterization

149 FT-IR spectra was recorded by fourier transform infrared spectroscopy (Perkin-Elmer,USA)
150 with KBr pellet and was used to investigate the chemical groups on the surface of MGO-MWCNTs,
151 MGO-MWCNTs/SMIP and MGO-MWCNTs/SNIP, and the results were shown in Fig. 3.



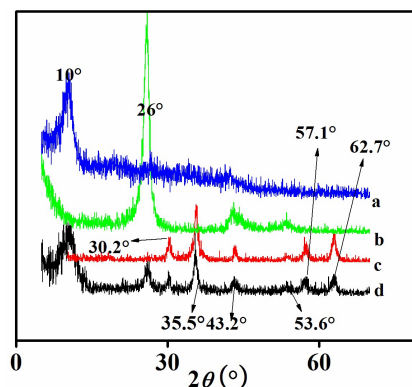
152

153 Fig. 3 The FT-IR spectrum of MGO-MWCNTs (a), MGO-MWCNTs/SMIP (b) and MGO-MWCNTs/SNIP (c).

154 In the spectrum of MGO-MWCNTs, the peak at 3445 cm^{-1} was the telescopic symmetrical
155 characteristic peak of $-\text{OH}$. 1735 cm^{-1} was the characteristic peak of carboxyl. The peak at 620 cm^{-1}
156 was the characteristic peak of Fe_3O_4 which gives evidence to the successful preparation of the
157 MGO-MWCNTs. In the spectrum of MGO-MWCNTs/SMIP, 1385 cm^{-1} (the characteristics of $-\text{CH}_3$),
158 1465 cm^{-1} (the characteristics of $-\text{CH}_2$) and 1533 cm^{-1} (the characteristics of $-\text{NH}-$) was able to
159 justify the preparation of the SMIP. Compared to MGO-MWCNTs/SNIP, the characteristic peak at
160 3000 cm^{-1} has an obvious displacement effected by hydrogen bonding. The results proved that
161 hydrogen bonding existed in synthesized SMIP.

162 X-ray diffraction (XRD) measurements were employed to investigate the phase and structures

163 of GO, MWCNTs, MGO-MWCNTs and Fe₃O₄. As shown in Fig. 4a, the GO show a characteristic
164 peak at $2\theta=10.9^\circ$ shown the GO was synthesized successfully [24]. Fig. 4b showed the typical XRD
165 patterns of the MWCNTs and the sharp peak was located at $2\theta=26^\circ$. The peaks in Fig. 4d at 2θ
166 values of 30.2° , 35.5° , 43.2° , 53.6° , 57.1° and 62.7° were consistent with the standard XRD data of
167 Fe₃O₄. All characteristic peaks of GO, MWCNTs and Fe₃O₄ were included in Fig. 4c which gives
168 evidences of the successful preparation of the MGO-MWCNTs.

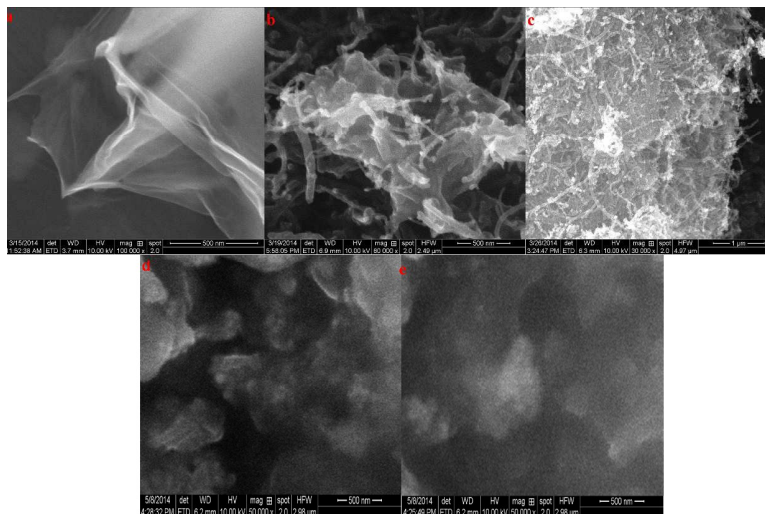


169

170

Fig. 4 XRD patterns of GO (a), MWCNTs (b), Fe₃O₄ (c) and MGO-MWCNTs (d).

171 Fig. 5 showed the SEM images of the obtained GO, GO-MWCNTs and MGO-MWCNTs. As
172 shown in Fig. 5, the GO (a) presents the sheet-like structure, smooth surface, and wrinkled edge. In
173 addition, GO and MWCNTs were uniformly intertwined as shown in Fig. 5b. It proved that
174 GO-MWCNTs were synthesized successfully, and Fe₃O₄ had coated on the GO-MWCNTs surface
175 as shown in Fig. 5c [25]. The MGO-MWCNTs/SMIP was shown in Fig. 5d and
176 MGO-MWCNTs/SNIP was shown in Fig. 5e are nano-particles, and roughness of the surface was
177 different. The MGO-MWCNTs/SMIP, it contains cavities of lysozyme, the surface of particles was
178 rough, and MGO-MWCNTs/SNIP was smooth without imprinted cavities. The
179 MGO-MWCNTs/SMIP was prepared with imprinted cavities.



180

181 Fig. 5 SEM images of the obtained GO (a), GO-MWCNTs (b), MGO-MWCNTs (c), MGO-MWCNTs/SMIP(d) and

182

MGO-MWCNTs/SMIP(e).

183

184

185

186

187

188

The BET surface area of MGO-MWCNTs/SMIP and MGO-MWCNTs/SMIP estimated from Barrett–Joyner–Halenda (BJH) analysis of the isotherms were determined. The surface area of MGO-MWCNTs/SNIP was 24.214 m²/g and the surface area of MGO-MWCNTs/SMIP was 57.295 m²/g. Obviously, the surface area of MGO-MWCNTs/SMIP was larger than that of MGO-MWCNTs/SNIP.

188

3.2 Adsorption study of MGO-MWCNTs/SMIP and MGO-MWCNTs/SNIP

189

190

191

192

193

194

195

196

197

198

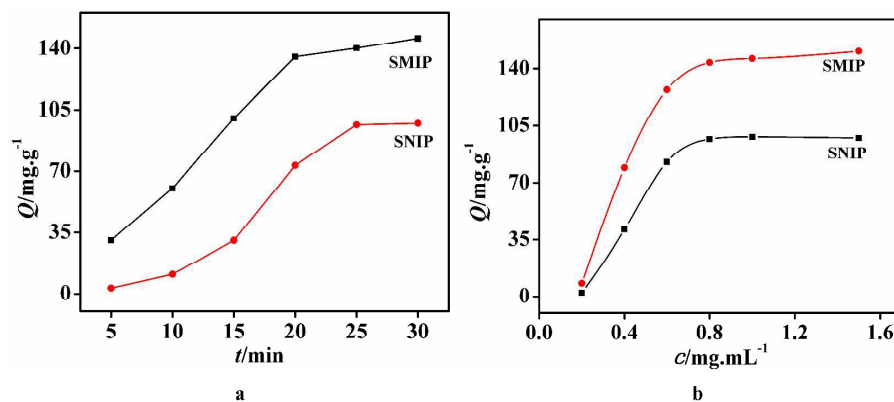
199

200

The adsorption property of MGO-MWCNTs/SMIP to lysozyme was shown in Fig. 6a. As it can be seen from the adsorption kinetics of MGO-MWCNTs/SMIP, lysozyme bounded to the polymers quickly at the beginning of adsorption. The adsorption amount of MGO-MWCNTs/SMIP increased and reached the maximum adsorption (140 mg/g) rapidly. At the beginning of adsorption, the hole of the SMIP could quickly capture the lysozyme molecule. When the most binding sites on the surface were occupied, the adsorption rate of SMIP to lysozyme decreased gradually due to the large steric hindrance. Similarly, the SNIP molecules adsorbed amount increased rapidly at the beginning stages of adsorption, but the adsorption capacity of SNIP was less than SMIP. The result can be explained that there were no specific recognition cavities to lysozyme in SNIP molecules.

Fig. 6b showed that the adsorption capacity of MGO-MWCNTs/SMIP molecules and MGO-MWCNTs/SNIP molecule, and the adsorption capacity increased with the increasing concentration of lysozyme. And when the concentration of lysozyme reached a certain concentration,

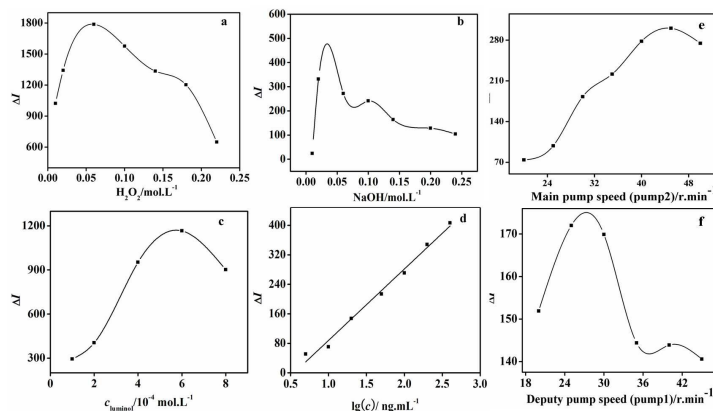
201 the adsorption capacity of the MGO-MWCNTs/SMIP and MGO-MWCNTs/SNIP would not increase.
 202 However, the adsorption capacity of MGO-MWCNTs/SNIP (95 mg/g) is much lower than the
 203 adsorption amount of MGO-MWCNTs/SMIP (140 mg/g). This is due to there is no imprinted
 204 cavities in MGO-MWCNTs/SNIP, only MGO and MWCNTs were involved in the adsorption of
 205 lysozyme. But, not only MGO and MWCNTs were involved in the adsorption of lysozyme in
 206 MGO-MWCNTs/SMIP, but also the MGO-MWCNTs/SMIP molecule has a specific recognition
 207 cavity for lysozyme, which makes the adsorption capacity of SMIP further increased. Therefore, the
 208 differences between MGO-MWCNTs/SMIP and MGO-MWCNTs/SNIP in adsorption appeared. In
 209 addition, a large hydrophobic groove (the active site of lysozyme) is present on the surface of
 210 lysozyme. And there are a large number of amino and carboxyl groups on the surface of lysozyme.
 211 So lysozyme can interact with many small molecules. Therefore, the nonspecific adsorption of
 212 lysozyme is serious and the adsorption capacity of MGO-MWCNTs/SMIP is only 50% higher than
 213 that of MGO-MWCNTs/SNIP.



214
 215 Fig. 6 The adsorption capacities of MGO-MWCNTs/SMIP and MGO-MWCNTs/SNIP.

216 3.3 Optimization of MGO-MWCNTs/SMIP-CL sensor

217 The diagram of FI-CL was shown in Fig. 1. The pump 2 speed, the pump 1 speed and
 218 concentrations of the luminescent reagents were optimized.



219
 220 Fig. 7 Optimization results. (a) Effect of H₂O₂ concentration on CL intensity. (b) Effect of NaOH concentration on CL intensity. (c)
 221 Effect of luminol concentration on CL intensity. (e) Effect of main pump (pump 2) speed on CL intensity. (f) Effect of deputy pump
 222 (pump 1) speed on CL intensity.

223 The experimental results were shown in Fig. 7. FI-CL signal was greatly affected by the
 224 concentration of H₂O₂ (Fig. 7a). With the H₂O₂ concentration in the range from 0.02 to 0.06 mol/L,
 225 the CL intensity reached maximum at the 0.05 mol/L concentration of H₂O₂. Thus, the optimum
 226 concentration of H₂O₂ was 0.05 mol/L.

227 The effect of concentration of NaOH solution on CL intensity was investigated in Fig. 7b. When
 228 NaOH concentration was in the scope of 0.01-0.24 mol/L, the CL intensity increased with the
 229 concentration of NaOH up to 0.03 mol/L. However, when the concentration of NaOH solution over
 230 0.03 mol/L, the CL intensity decreased. Thence, 0.03 mol/L was the ideal choice as the concentration
 231 of NaOH solution.

232 The influence of concentration of luminol solution was examined over the range of 1.0×10^{-4} -
 233 8.0×10^{-4} mol/L, the CL intensity reached maximum when the concentration of luminol was 6.0×10^{-4}
 234 mol/L as shown in Fig. 7c.

235 The effect of main pump (pump 2) speed on luminous intensity was explored in Fig. 7e. As we
 236 can observed, the optimal pump speed of pump 2 was 45 r.min⁻¹.

237 The deputy pump (pump1) speed was studied on CL intensity. As shown in Fig. 7f. The optimal
 238 pump speed of pump 1 was 25 r.min⁻¹.

239 3.4 Analytical performance of sensor

240 Under the optimum conditions, the linearly response range of the sensor for lysozyme was
 241 obtained as shown in Fig. 7d. The linear equation expressed as $\Delta I = -1.14 \times 10^2 + 1.99 \times 10^2 \lg c$ (c was the
 242 lysozyme concentration) and the correlation coefficient was 0.9950. The detection limit was
 243 1.90×10^{-9} g/mL and the sensor responded linearly to the lysozyme over the range 5.04×10^{-9} -

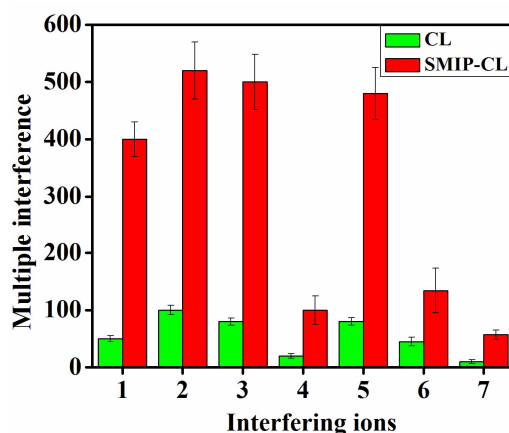
244 4.27×10^{-7} g/mL. Thence, it is proved that the method has low detection limit.

245 Then the sensor was placed in a vacuum oven. Two weeks later, the sensor was used to detect
246 lysozyme and the sensor performance did not change significantly. The RSD was within the
247 acceptable range. Therefore, the sensor was in good stability.

248 3.5 Interferences study

249 Under the exploring conditions (luminol: 6.0×10^{-4} mol/L, NaOH: 0.03 mol/L, H_2O_2 : 0.05 mol/L,
250 pump 2 speed: 45 r/min, the pump 1 speed: 25 r/min). Coexisting substances was added into
251 lysozyme solution (3.0×10^{-8} mol/L⁻¹) to investigate the effect on CL intensity. variety of substances
252 were added into lysozyme solution to examine the effects for determination the lysozyme. The
253 tolerable fold of interfering substances in sample with MGO-MWCNTs/SMIP and
254 MGO-MWCNTs/SNIP column was compared when relative error was less than $\pm 5\%$ and the
255 tolerance times are shown in Fig. 8.

256 These result showed that after MGO-MWCNTs/SMIP was used to sensor, the detection of
257 lysozyme was not affected by 400 times the concentration of Fe^{3+} , 520 times the concentration of
258 Na^+ , 500 times the concentration of citric acid, 100 times the concentration of cytochrome C, 480
259 times the concentration of lactate, 130 times the concentration of bovine serum albumin and 50 times
260 the concentration of bovine hemoglobin. The anti-jamming capability of sensor was increased
261 obviously. Thus, the sensor could be used to lysozyme analysis and the selectivity has been increased
262 dramatically.



263

264 Fig. 8 Interference study. 1: Fe^{3+} ; 2: Na^+ ; 3: citric acid; 4: cytochrome C; 5: lactate; 6: bovine serum albumin; 7: bovine hemoglobin.

265 3.6 Application of MGO-MWCNTs/SMIP-CL sensor

266 The sensor was used to detect lysozyme in eggs. Egg samples need to be processed before: the

267 egg was cracked and egg white was diluted by PBS (pH=7.47, c : 0.01 mol/L). The solution was
268 bathed at 77 °C for 10min and was centrifuged in order to obtain the supernatant. Then, the
269 supernatant was diluted tenfold. And according to the test method, the spiked recovery experiment
270 was carried out.

271 The result was shown in Table 1. The recoveries varied from 98% to 111%. As a result, the CL
272 sensor used for the determination of lysozyme was practical.

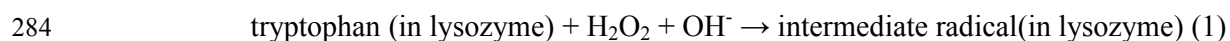
273 Table 1 Determination results of samples ($n=6$).

Samples	Content(ng/mL)	Added(ng/mL)	Found(ng/mL)	Recovery(%)	RSD(%)
1 [#]	200	100	311	111	3.4
2 [#]	100	100	198	98	3.7
3 [#]	50	100	156	106	4.1

274 3.7 Possible mechanism of the reaction

275 The structure of lysozyme consists of α - helix, β - fold, β - corner and random coil. And the
276 lysozyme was a globular protein contained 129 tactic amino acid residues with the active center in
277 the cleft between the two domains on the molecule surface[26].Six tryptophan residues are located at
278 the binding site of lysozyme and the 62th and 108th of the tryptophan residues are burned the main
279 groups.

280 In view of the widespread use of H_2O_2 in protein modification, the mechanism of H_2O_2
281 oxidizing certain amino acids in lysozyme is not clear up to now. However, Song [27] has proved
282 that lysozyme can enhance the chemiluminescence signal and the possible mechanism of the reaction
283 was proposed. Therefore, it may be concluded that the enhancement mechanism is presented below:



286 Conclusions

287 In this work, the MGO-MWCNTs/SMIP which exhibited high selectivity to lysozyme was
288 synthesized. The MGO-MWCNTs/SMIP was characterized by SEM, XRD and FT-IR. The
289 adsorption properties of the polymer were studied. Then, a new CL method for the determination of
290 lysozyme based on SMIP was achieved. Luminol-NaOH- H_2O_2 CL system was selected and the
291 optimum condition for CL was explored. The proposed method responded linearly to the
292 concentration of lysozyme over the range was 5.04×10^{-9} - 4.27×10^{-7} g/mL. The detection limit was

293 1.90×10^{-9} g/mL (3δ) which reflected the sensor was satisfactory. The advantageous properties of
294 sensor hold the potential to be applied in protein analysis, analogizing to biological analysis.

295 **Acknowledgment**

296 This work was supported by the National Natural Science Foundation of China (NSFC, Nos.
297 21345005 and 21205048), the Shandong Provincial Natural Science Foundation of China (No.
298 ZR2012BM020) and the Scientific and technological development Plan Item of Jinan City in China
299 (No. 201202088).

300 **References**

- 301 [1] Mai, W.; Hu, C. cDNA cloning, expression and antibacterial activity of lysozyme C in the blue
302 shrimp (*Litopenaeus stylirostris*). *Progress in Natural Science*, 2009, 19: 837-844.
- 303 [2] Cheng, A.; Ge, B.; Yu, H. Aptamer-based biosensors for label-free voltammetric detection of
304 lysozyme. *Analytical Chemistry*, 2007, 79: 5158-5164.
- 305 [3] Sun, N.; Chen, S.; Xie, X.; Wang, Y.; Li, G, et al. Expression, characterization and antimicrobial
306 ability of a variant T4 lysozyme in *pichia pastoris*. *Agricultural Science Technology*, 2014, 15:
307 321-325.
- 308 [4] Ren, Q.; Zhao, X.; Wang, J. Molecular characterization and expression analysis of a chicken-type
309 lysozyme gene from housefly (*Musca domestica*). *Journal of Genetics and Genomics*, 2009, 36:
310 7-16.
- 311 [5] Wang, N.; Wang, Y.; Li, G.; Sun, N. Expression, characterization and antimicrobial ability of T4
312 lysozyme from methylotrophic yeast *hansenula polymorpha* A16. *Science China Life Sciences*,
313 2011, 54: 520-526.
- 314 [6] Morita, S.; Kuriyama, M.; Nakatsu, M.; Suzuki, M.; Kitano, K. Secretion of active human
315 lysozyme by *acremonium chrysogenum* using a *fusarium* alkaline protease promoter system.
316 *Journal of Biotechnology*, 1995, 42: 1-8.
- 317 [7] Osserman, E.; Klockars, M.; Halper, J.; Fischel, E. Effects of lysozyme on normal and
318 transformed mammalian cells. *Nature*, 1973, 243: 331-335.
- 319 [8] Warren, J.; Rinehart, J.; Zwilling, B.; Neidhart, J. Lysozyme enhancement of tumor cell
320 immunoprotection in a murine fibrosarcoma. *Cancer Research*, 1981, 41: 1642-1645.

- 321 [9] Wooley, R.; Schall, W.; Eagon, R. Efficacy of EDTA-Tris-lysozyme lavage in the treatment of
322 experimentally in induced pseudomonas aeruginosa cystitis in the dog. American Journal of
323 Veterinary Research, 1974, 35: 27-29.
- 324 [10] Durance, T.; Timothy, D. Process for isolation of lysozyme and avidin from egg white. US 4,
325 996, 851. October 30, 1990.
- 326 [11] Pasternack, R.; Collings, P. Resonance light-scattering-A new technique for studying
327 chromophore aggregation. Science, 1995, 269: 935-939.
- 328 [12] Pasternack, R.; Bustamante, C.; Collings, P.; Giannetto, A.; Gibbs, E. Porphyrin assemblies on
329 DNA as studied by a resonance light-scattering technique. Journal of the American Chemical
330 Society, 1993, 115: 5393-5399.
- 331 [13] Deng, H.; Gao, L.; Zhang, S.; Yuan, J. Preparation of a copper ion selective membrane by
332 surface-modified molecular imprinting. Industrial and Engineering Chemistry Research. 2012,
333 51: 14018-14025.
- 334 [14] Zayats, M.; Kanwar, M.; Ostermeier, M.; Searson, P. Molecular imprinting of maltose binding
335 protein: tuning protein recognition at the molecular level. Macromolecules, 2011, 44,: 3966.
- 336 [15] Behzad, H.; Somayyeh, B. Flow injection chemiluminescence determination of isoniazid using
337 luminol and silver nanoparticles. Microchemical Journal, 2010, 95: 192–197
- 338 [16] Tsukago, K.; Sumiyama, M.; Naka, J. Chemilu-minescence property of the luminol-hydrogen
339 peroxide-copper system in the presence of surface-carboxylated microspheres. Analytical
340 Sciences, 1998, 14: 409-412.
- 341 [17] Rezaei, B.; Mokhtari, A. A simple and rapid flow injection chemiluminescence determination of
342 cysteine with $\text{Ru}(\text{phen})_2^+-\text{Ce}(\text{rV})$ system. Spectrochimica Acta Part A: Molecular and
343 Biomolecular Spectroscopy, 2007, 66: 359-363.
- 344 [18] Liu, J.; Zhang, L.; Wang, Y.;Zheng, Y.; Sun, S. An improved portable biosensing system based
345 on enzymatic chemiluminescence and magnetic immunoassay for biological compound
346 detection. Measurement, 2014, 47: 200-206.
- 347 [19] Yao, H.; Xu, E.; Zeng, W.; Zeng, X.; Zhang, M, et al.Determination of doxorubicin in
348 pharmaceutical preparation and rat plasma with luminol- $\text{K}_3\text{Fe}(\text{CN})_6$ chemiluminescence system.
349 Journal of Food and Drug Analysis, 2013, 21: 279-285.

- 350 [20] Tan, X.; Wang, Z.; Chen, D.; Luo, K.; Song, Z, et al. Study on the interaction of catalase with
351 pesticides by flow injection chemiluminescence and molecular docking. *Chemosphere*, 2014,
352 108:26-32.
- 353 [21] Hummers, W.; Offeman, R. Preparation of graphitic oxide. *Journal of the American Chemical*
354 *Society*. 1958, 80: 1339.
- 355 [22] Qin, X.; Wang, H.; Wang, X.; Miao, Z.; Chen, L, et al. Amperometric biosensors based on gold
356 nanoparticles-decorated multiwalled carbon nanotubes-poly(diallyldimethylammonium chloride)
357 biocomposite for the determination of choline. *Sensors and Actuators B: Chemical*, 2010, 147:
358 593-598.
- 359 [23] Qiu, H.; Luo, C.; Sun, M.; Lu, F.; Fan, L, et al. A chemiluminescence array sensor based on
360 graphene-magnetite-molecularly imprinted polymers for determination of benzenediol isomers.
361 *Analytica Chimica Acta*, 2012, 744: 75-81.
- 362 [24] Han, D.; Yan, L.; Chen, W.; Li, W. Preparation of chitosan/graphene oxide composite film with
363 enhanced mechanical strength in the wet state. *Carbohydr Polym*, 2011, 83: 653-8.
- 364 [25] Qiu, H.; Luo, C.; Sun, M.; Lu, F.; Fan, L, et al. Determination of L-tryptophan based on
365 grapheneoxide–magnetite-molecularly imprinted polymers and chemiluminescence. *Talanta*,
366 2012, 98: 226-230.
- 367 [26] Wang, Z.; Song, Z. A valuable way for understanding the relationships between lysozyme and
368 cephalosporin analogues by flow injection chemiluminescence. *Analyst*, 2010, 135: 2546-2553.
- 369 [27] Song, Z.; Hou, S. A new analytical procedure for assay of lysozyme in human tear and saliva
370 with immobilized reagents in flow injection chemiluminescence system. *Analytical Sciences*
371 2003, 19: 347-352.